

A Mathematical Study of COVID-19 Outbreak with Uncertainties of Controlling Parameters

Prasenjit Mahato¹, Sanat Kumar Mahato² and Subhashis Das³

^{1,2,3}Department of Mathematics, Sidho-Kanho-Birsha University, Purulia – 723104, West Bengal, India

¹pmmath1994@gmail.com*, ²sanatkmahato@gmail.com, ³dassubhashis409@gmail.com

¹ORCID ID - 0000-0002-4572-0699, ²ORCID ID - 0000-0001-5455-5173,

³ORCID ID - 0000-0002-4273-7241

Received: 30.09.2021; accepted: 09.12.2021; published online: 30.12.2021

Rapidly spreading disease, COVID-19 is classified as the human-to-human transmissible disease and currently it becomes a pandemic in the Globe. In this paper, we propose the conceptual mathematical model and analyze a Susceptible-Exposed-Infected-Quarantined or Isolated-Recovered-Susceptible (SEIRUS) type infectious disease model with imprecise parameters. We have divided the model formulation portion into four subsections. They are namely crisp SEIRUS model, interval SEIRUS model and fuzzy SEIRUS model. The existence condition and boundedness of the solution to our proposed model have been discussed. The asymptotical stability of the system at different equilibrium point is investigated. Also we have explained the global stability at endemic equilibrium point. Application of optimal control of the system is described and solved. Finally, some numerical results have been shown to test the theoretical study of the model. We observed that the population is greatly influenced for the imprecise nature of parameters.

Key words: COVID-19 coronavirus, SEIRUS model, imprecise parameter, Reproduction number, Stability, Optimal control

Background

The emergence of infectious disease is important factors that cause the mortality of human and animal as well as social and economic breakdown [10, 32, 49]. Infectious disease can govern the population size, population dynamics [27, 45], and their host population [1, 13, 15, 37]. In the field of epidemiological mathematics we measure the investigation by Murray [33] and Hethcote [14] as pathfinder. Epidemics affected the world the Zika virus outbreak in Brazil in 2014, Ebola outbreak in West Africa in 2014–2016, HIV in West Africa in late 20th century, American Plagues in 16th century, Great Plague of London around 1665–1666, Russian plague around 1770–1772, Philadelphia yellow fever epidemic in 1793, outbreak of Black Death in London around 1665–1666, plague in Mumbai in 1906. Some studies [29, 42, 44] described logistic growth model. The disease dynamics of tuberculosis with non local conformable derivative have been discussed by Khan and Gomez-Aguilar [22]. Hospital transmission is main issue in epidemic syndrome which has been studied by Riley et al. [43] in their work. Many

researchers considered that the process of reproduction of epidemic caused by virus is prime issue [30]. Chavez et al.[6] have studied mathematical models for disease dynamics of tuberculosis. The construction of next generation matrices for epidemic model was developed by Diekmann et al. [9]. The dynamics of Zika virus with Lyapunov function theory was described by some researcher [23]. Khan et al. [24] have described the intercourse of infected from symptomatic stage to asymptomatic stage in HIV/AIDS infection. Study by Njankou et al. [38] is about the optimal control of Ebola virus disease. They considered three different control measures such as education campaigns, active case searching and pharmaceutical interventions.

Main findings The main finding of this work is to improve new mathematical model, called SEIRUS model in fuzzy environment. Combining strict lock down, widespread testing, quarantine or isolation as precautionary measure is the key of rapidly ending the COVID-19 pandemic.

1. Introduction

Coronavirus disease was first marked off in December 2019 in Wuhan, China and it has been breaking out throughout the world. The symptoms of the COVID-19 are commonly weariness, fever, dry

*Corresponding author Email id:
pmmath1994@gmail.com

cough. Many patients also give symptoms such as sore throat, anosmia, ageusia, nausea, vomiting, diarrhea, shortness of breath, aches, nasal congestion. It is the higher risk for the old patients for some lethal diseases such as coronary heart disease, diabetes and hypertension.

COVID-19 which is a contagious disease causes mainly the respiratory syndrome and transmissible from human-to-human [3, 18]. At this situation more than 210 countries and territories have reported to have coronavirus patients and its infection increase explicatively [26]. The primary host was found in animals and disposed to humans [2]. Nesteruk et al. [36] in his SIR (Susceptible-Infectious-Removed) model suggested the good values statistically for model parameters. Ming et al. [34] and Oduwole et al. [39] discussed how to control the disease through his model. Wu et al. [50] have displayed a susceptible exposed infectious recovered model (SEIR) model. The disease dynamics and its transmission and portending for the national and global disease spread is the main substance of his work. Tang et al. [46] has considered in his study with a separated deterministic model formation with the disease's clinical improvement. The epidemic trajectories on computational modeling with estimation the size of the spread of the disease in Wuhan is performed by Imai et al. [19]. They have discussed the diseases transmission from human to human. Mathematical modeling is broadly used for forecasting the results of an epidemic successfully in the study of epidemiology. SIS, SIR and SEIR models are mostly common used in the epidemiological research work. The Kermack-Mckendric SIR model is a very well initiated model and used largely for various epidemics [25, 48]. We have not found any visible symptoms to infected individuals as for example chicken pox, tuberculosis in any other cases. In that cases an SEIR model is vastly used [26]. Khajanchi et al. [21] have formed the SAIUQR model. They have explained the forecasting the daily and cumulative number of cases for the COVID 19 pandemic in India. Giordano et al. [12] have studied on SIDARTHE model. They have to special emphasis on population testing. It has been suggested that testing is the most urgent as undetected infected people most of them asymptomatic and they are huge sustain the epidemic spread. Also they have explained for maintaining strict lockdown and to increase widely testing to the population and contact tracing effort significantly. Pal et al. [41] discussed COVID-19 epidemic model using data driven epi-

demiological parameters in India. We use uncertainty for the associated parameters uncertain to form more realistic model. So we may use the uncertain interval valued parameter. It may help to inform a real world mathematical system. Zadeh [51] first used the uncertainty in his mathematical deduction. The application of Fuzzy set theory along with interval valued parameters has been vastly used in various research fields. Mahato et al. [40] have used the fuzzy in his epidemic model. They have assumed the fuzzy value of infected human population and fuzzy basic reproductive number and taken uncertainty parameters. Researchers paid attention to develop their epidemic models in uncertain environments [5, 7, 28, 31, 35, 55, 56, 57, 58] such as fuzzy, interval, stochastic, intuitionistic fuzzy, etc. The reason to consider the uncertain environment is that in reality data cannot be collected precisely due to several causes like fluctuation of environment, changes in the nature of the virus, ambiguous death rate such as co-morbidity death, uncertainty about the number of undetected infections etc. To avoid uncertainty and variations, Efimov [11] developed an interval prediction of COVID-19 based SEIR epidemic model.

The paper is embodied as follows: Some useful definitions are presented in section 2. Mathematical Model is discussed with elaboration in section 3. Positivity and boundedness of the system, stability criteria of disease free equilibrium and endemic equilibrium are prescribed in the section of 4. Optimality of system of the crisp model is described in section 5. Section 6 is accomplished with the sensitivity analysis of parameters. Some numerical examples are explained graphically in section 7. Numerical results with control policies are investigated in section 8. Finally, section 9 outlines conclusion of the results.

2. Some Useful Definitions

In this section, we give some useful definitions. These definitions or properties are used throughout the work. They are defined in the following way.

2.1 Interval number

The closed interval $[\underline{p}, \bar{q}]$ represents an interval number S and defined as following

$$S = [\underline{p}, \bar{q}] = \{x : \underline{p} \leq x \leq \bar{q}, x \in \mathcal{R}\}$$

where \mathcal{R} is the set of real number and \underline{p} and \bar{q} are the upper and lower limit interval number respectively.

2.2 Interval valued function

We represent an interval valued function with parametric form. We define the interval $[m, n]$ by the following function

$$f(\alpha) = m^{1-\alpha} \cdot n^\alpha, \alpha \in [0, 1].$$

Then the operation (\circ) for two interval numbers can be written as

$$\{(\underline{m})^{1-\alpha}(m)^\alpha\} \circ \{(\underline{n})^{1-\alpha}(n)^\alpha\} = (\underline{z})^{1-\alpha}(\bar{z})^\alpha.$$

where, $\underline{z} = \min\{\underline{m} \circ \underline{n}, \overline{m} \circ \underline{n}, \underline{m} \circ \overline{n}, \overline{m} \circ \overline{n}\}$ and $\bar{z} = \max\{\underline{m} \circ \underline{n}, \overline{m} \circ \underline{n}, \underline{m} \circ \overline{n}, \overline{m} \circ \overline{n}\}$

2.3 Fuzzy Number

A fuzzy set \tilde{A} is called a fuzzy number with membership function $\mu_{\tilde{A}}(l)$ if it is normal and convex, i.e.,

- (i) $\mu_{\tilde{A}}(l_0) = 1$ for some l_0 ,
- (ii) $\mu_{\tilde{A}}(\lambda l_1 + (1-\lambda)l_2) \leq \lambda\mu_{\tilde{A}}(l_1) + (1-\lambda)\mu_{\tilde{A}}(l_2)$

Now, GMIV of $\tilde{A} = 2 \int_0^1 p\{(1-q)L^{-1}(p) + qR^{-1}(p)\}dp$

$$= 2 \int_0^1 p\{(1-q)[a_1 + (a_2 - a_1)p] + q[a_3 - (a_3 - a_2)p]\}dp$$

$$= 2 \left[(1-q) \left\{ \frac{a_2}{2} + \frac{(a_2 - a_1)p}{3} \right\} + q \left\{ \frac{a_3}{2} - \frac{(a_3 - a_2)}{3} \right\} \right]$$

$$= \frac{1}{3}[(1-q)a_1 + 2a_2 + qa_3]$$

Thus, $D_f(\tilde{A}) = \frac{1}{3}[(1-q)a_1 + 2a_2 + qa_3]$.

If $a_1 = a_2 = a_3 = a$, then $\tilde{A} = (a, a, a)$ reduced to the real number ‘a’.

2.4 Defuzzification Method

In the year 1999, Chen and Hsieh [8], proposed a defuzzification method known as graded mean integral value method and is given by

$$D_f(\tilde{A}) = \frac{\int_0^1 p\{(1-q)L^{-1}(p) + qR^{-1}(p)\}dp}{\int_0^1 pdp}$$

$$= 2 \int_0^1 p\{(1-q)L^{-1}(p) + qR^{-1}(p)\}dp$$

where, $L(p)$ and $R(p)$ are the left and right shape functions of the fuzzy number \tilde{A} respectively and $q \in [0, 1]$ is the degree of optimism.

2.5 GMIV of Triangular Fuzzy Number (TFN)

The left and right shape functions of the TFN \tilde{A} are respectively, $L(p) = \frac{p-a_1}{a_2-a_1}$ and $R(p) = \frac{a_3-p}{a_3-a_2}$. Therefore, $L^{-1}(p) = a_1 + (a_2 - a_1)p$ and $R^{-1}(p) = a_3 - (a_3 - a_2)p$

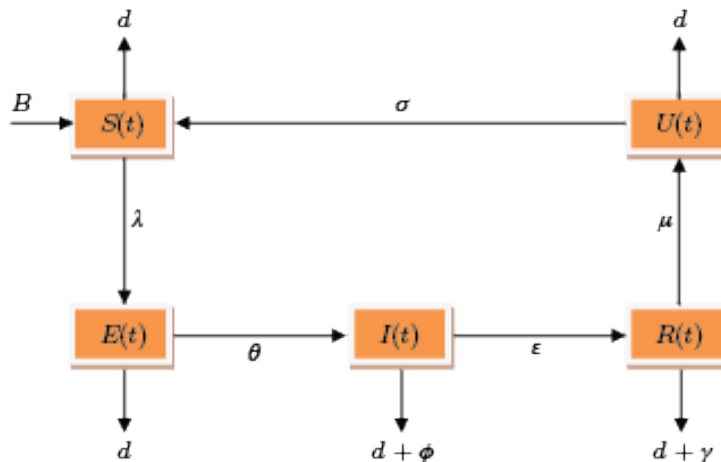


Fig. 1. The Schematic Diagram of the proposed model

3. Model Formulation

3.1 Model 1: Crisp SEIRUS Model

In this paper we formulate and analyze a SEIRUS type epidemic model. It is assumed that the variables are $S(t)$, $E(t)$, $I(t)$, $R(t)$, $U(t)$ i.e. number of the susceptible population, number of the exposed population, number of the infected population, number of quarantined or isolated population and number of the recovered population respectively at any instant of time t .

We assume that the total recruitment rate of human population is B . According to the different form of disease transmission we have considered the disease transmitted to the susceptible population when an infected population comes into contiguity of the susceptible individuals with λ be the disease transmission rate. Therefore λSI part moves on the exposed class from the susceptible class. We have treated that d is the natural death rate of all the individuals and Θ be considered the force of infection in the population, ϵ is the proportion of the infected population in quarantine time per unit time and φ is to be disease induced death rate of infected population who are not quarantined or isolated. Again, we assume γ to be disease induced death rate of infected population who are quarantined or isolated and σ is the proportion of observed population and being moved to susceptible class. We also assume that μ is the recovery rate of the quarantined or isolated population at any time t . Then the dynamical behavior of this pandemic caused by the infection and the situation thereafter can be illustrated by the following system of nonlinear ordinary differential equation.

$$\begin{aligned} \frac{dS(t)}{dt} &= B - \lambda SI - dS + \sigma U \\ \frac{dE(t)}{dt} &= \lambda SI - dE - \Theta E \end{aligned}$$

$$\begin{aligned} \frac{dS(t, \alpha)}{dt} &= (\underline{B})^{1-\alpha}(\overline{B})^\alpha - (\underline{\lambda})^{1-\alpha}(\overline{\lambda})^\alpha SI - (\underline{d})^{1-\alpha}(\overline{d})^\alpha S + (\underline{\sigma})^{1-\alpha}(\overline{\sigma})^\alpha U \\ \frac{dE(t, \alpha)}{dt} &= (\underline{\lambda})^{1-\alpha}(\overline{\lambda})^\alpha SI - (\underline{d})^{1-\alpha}(\overline{d})^\alpha E - (\underline{\Theta})^{1-\alpha}(\overline{\Theta})^\alpha E \\ \frac{dI(t, \alpha)}{dt} &= (\underline{\Theta})^{1-\alpha}(\overline{\Theta})^\alpha E - [(\underline{d})^{1-\alpha}(\overline{d})^\alpha + (\underline{\epsilon})^{1-\alpha}(\overline{\epsilon})^\alpha + (\underline{\varphi})^{1-\alpha}(\overline{\varphi})^\alpha] I \\ \frac{dR(t, \alpha)}{dt} &= (\underline{\epsilon})^{1-\alpha}(\overline{\epsilon})^\alpha I - [(\underline{d})^{1-\alpha}(\overline{d})^\alpha + (\underline{\mu})^{1-\alpha}(\overline{\mu})^\alpha + (\underline{\gamma})^{1-\alpha}(\overline{\gamma})^\alpha] R \\ \frac{dU(t, \alpha)}{dt} &= (\underline{\mu})^{1-\alpha}(\overline{\mu})^\alpha R - [(\underline{d})^{1-\alpha}(\overline{d})^\alpha + (\underline{\sigma})^{1-\alpha}(\overline{\sigma})^\alpha] U \end{aligned} \tag{2}$$

where $\alpha \in [0, 1]$, α depends on the environment.

$$\begin{aligned} \frac{dI(t)}{dt} &= \Theta E - (d + \epsilon + \varphi)I \\ \frac{dR(t)}{dt} &= \epsilon I - (d + \mu + \gamma)R \\ \frac{dU(t)}{dt} &= \mu R - (d + \sigma)U \end{aligned} \tag{1}$$

with the condition $S(t) \geq 0$, $E(t) \geq 0$, $I(t) \geq 0$, $R(t) \geq 0$, $U(t) \geq 0$.

3.2 Model 2: Interval SEIRUS Model

For interval approach we do not need any membership, non membership or probability distribution function but we can vary the parameters in some suitable range. For the reason we have used the interval approach. We treat all parameters as interval numbers then system of equation (1) reduces in following form:

$$\begin{aligned} \frac{\widehat{dS}}{dt} &= \widehat{B} - \widehat{\lambda}SI - \widehat{d}S + \widehat{\sigma}U \\ \frac{\widehat{dE}}{dt} &= \widehat{\lambda}SI - \widehat{d}E - \widehat{\Theta}E \\ \frac{\widehat{dI}}{dt} &= \widehat{\Theta}E - (\widehat{d} + \widehat{\epsilon} + \widehat{\varphi}) \\ \frac{\widehat{dR}}{dt} &= \widehat{\epsilon}I - (\widehat{d} + \widehat{\mu} + \widehat{\gamma})R \\ \frac{\widehat{dU}}{dt} &= \widehat{\mu}R - (\widehat{d} + \widehat{\sigma})U \end{aligned}$$

where, $\widehat{B} = [\underline{B}, \overline{B}]$, $\widehat{\lambda} = [\underline{\lambda}, \overline{\lambda}]$, $\widehat{d} = [\underline{d}, \overline{d}]$, $\widehat{\epsilon} = [\underline{\epsilon}, \overline{\epsilon}]$, $\widehat{\sigma} = [\underline{\sigma}, \overline{\sigma}]$, $\widehat{\Theta} = [\underline{\Theta}, \overline{\Theta}]$, $\widehat{\varphi} = [\underline{\varphi}, \overline{\varphi}]$, $\widehat{\mu} = [\underline{\mu}, \overline{\mu}]$, $\widehat{\gamma} = [\underline{\gamma}, \overline{\gamma}]$.

The above equation can be written in parametric form as follows

3.3 Model 3: Fuzzy SEIRUS Model

In this portion, we consider parameters as fuzzy number. Then the system of differential equations given in (1) is transformed into the following system of differential equation.

$$\begin{aligned}
 \frac{d\widetilde{S}(t)}{dt} &= \widetilde{B} - \widetilde{\lambda}SI - \widetilde{d}S + \widetilde{\sigma}U \\
 \frac{d\widetilde{E}(t)}{dt} &= \widetilde{\lambda}SI - \widetilde{d}E + \widetilde{\theta}E \\
 \frac{d\widetilde{I}(t)}{dt} &= \widetilde{\theta}E - (\widetilde{d} + \widetilde{\epsilon} + \widetilde{\varphi})I \\
 \frac{d\widetilde{R}(t)}{dt} &= \widetilde{\epsilon}I - (\widetilde{d} + \widetilde{\mu} + \widetilde{\gamma})R \\
 \frac{d\widetilde{U}(t)}{dt} &= \widetilde{\mu}R - (\widetilde{d} + \widetilde{\sigma})U
 \end{aligned} \tag{3}$$

We take all the parameters positive. i.e. $\widetilde{B} > 0$, $\widetilde{\lambda} > 0$, $\widetilde{d} > 0$, $\widetilde{\epsilon} > 0$, $\widetilde{\sigma} > 0$, $\widetilde{\theta} > 0$, $\widetilde{\varphi} > 0$, $\widetilde{\mu} > 0$, $\widetilde{\gamma} > 0$ and consider them as triangular fuzzy numbers. With the help of graded mean integration defuzzification method, we convert the fuzzy model system of equation in the following way:

$$\begin{aligned}
 D_f\left(\frac{d\widetilde{S}(t)}{dt}\right) &= D_f(\widetilde{B}) \\
 &\quad - D_f(\widetilde{\lambda})SI - D_f(\widetilde{d})S + D_f(\widetilde{\sigma})U \\
 D_f\left(\frac{d\widetilde{E}(t)}{dt}\right) &= D_f(\widetilde{\lambda})SI - D_f(\widetilde{d})E - D_f(\widetilde{\theta})E \\
 D_f\left(\frac{d\widetilde{I}(t)}{dt}\right) &= D_f(\widetilde{\theta})E - (D_f(\widetilde{d}) \\
 &\quad + D_f(\widetilde{\epsilon}) + D_f(\widetilde{\varphi}))I \\
 D_f\left(\frac{d\widetilde{R}(t)}{dt}\right) &= D_f(\widetilde{\epsilon})I - (D_f(\widetilde{d}) \\
 &\quad + D_f(\widetilde{\mu}) + D_f(\widetilde{\gamma}))R \\
 D_f\left(\frac{d\widetilde{U}(t)}{dt}\right) &= D_f(\widetilde{\mu})R - (D_f(\widetilde{d}) + D_f(\widetilde{\sigma}))U
 \end{aligned}$$

Here, D_f is defuzzification operator and $D_f(\cdot)$'s the defuzzified/GMIV parameter.

4. Theoretical Study of the Model

Here, we have analyzed the theoretical study of the proposed dynamic system. We have investigated the positivity, boundedness of the model, basic reproduction number and the stability criteria of the system.

4.1 Positivity of the model

Theorem 1: Solutions of the model (1) are non negative starting from R_+^5 .

Proof: With the help of crisp model (1), we have

$$\begin{aligned}
 \frac{dS(t)}{dt}\Big|_{S=0} &= B + \sigma U, \\
 \frac{dE(t)}{dt}\Big|_{E=0} &= \lambda SI, \\
 \frac{dI(t)}{dt}\Big|_{I=0} &= \theta E, \\
 \frac{dR(t)}{dt}\Big|_{R=0} &= \epsilon I, \\
 \frac{dU(t)}{dt}\Big|_{U=0} &= \mu R.
 \end{aligned}$$

From above, we have got that all the rates are non negative in a bounding planes of non negative cone of R_+^5 . If, we draw the direction of the vector field which is inward on the entire bounded planes. So all the solutions of the system (1) are non negative in R_+^5 .

4.2 Boundedness of the system

Theorem 2: The solutions of the model (1) are uniformly bounded.

Proof: Let us consider an auxiliary variable representing the sum of all classes

$$\begin{aligned}
 X &= S + E + I + R + U \\
 \frac{dX}{dt} &= \frac{dS}{dt} + \frac{dE}{dt} + \frac{dI}{dt} + \frac{dR}{dt} + \frac{dU}{dt} \\
 \frac{dX}{dt} + dX &= B - \varphi I - \gamma R \\
 \frac{dX}{dt} + dX &\leq B
 \end{aligned}$$

We integrate both side with respect to t with the help of the theory of differential inequality due to Brikhoff and Rota [4]. Then we have the following results

$$0 < X(S, E, I, R, U) \leq \frac{B}{d} \text{ as } t \rightarrow \infty$$

So, all the solution of the system (1) initiated at $[R_+^5 \setminus 0]$ are confined in the following range

$$\mathcal{R} = \{(S, E, I, R, U) \in R_+^5 : X = \frac{B}{d} + \epsilon\}$$

for any $\epsilon > 0$ and $t \rightarrow \infty$

Therefore, we may determine that all the solutions of the above system (1) are positive and uniformly bounded.

Theorem 3: The solutions of the interval model given in equation (2) are uniformly bounded in the region $\mathcal{R} = \left\{ (S, E, I, R, U) \in R_+^5 : N = \frac{(\underline{B})^{(1-\alpha)}(\overline{B})^\alpha}{(\underline{d})^{(1-\alpha)}(\overline{d})^\alpha} + \epsilon \right\}$, for any $\epsilon > 0$ and for $t \rightarrow \infty$.

Theorem 4: The solutions of the fuzzy model given in equation (3) are uniformly bounded in the region $\mathcal{R} = \left\{ (S, E, I, R, U) \in R_+^5 : N = \frac{D_f(\tilde{B})}{D_f(\tilde{d})} + \epsilon \right\}$, for any $\epsilon > 0$ and for $t \rightarrow \infty$.

Now we apply the next generation matrix method [47] on the system of (1) and compute the basic reproduction number (R_0). The spectral radius of the matrix $(F \cdot V_1^{-1})$ or R_0 is computed as

$$R_0 = \frac{\lambda\Theta B}{d(d + \Theta)(d + \epsilon + \varphi)}$$

. For interval SEIRUS model and fuzzy SEIRUS model, the basic reproduction number can be written as respectively

$$R_{0h} = \frac{(\underline{\lambda})^{1-\alpha}(\overline{\lambda})^\alpha(\underline{\Theta})^{1-\alpha}(\overline{\Theta})^\alpha(\underline{B})^{1-\alpha}(\overline{B})^\alpha}{(\underline{d})^{1-\alpha}(\overline{d})^\alpha \{(\underline{d})^{1-\alpha}(\overline{d})^\alpha + (\underline{\Theta})^{1-\alpha}(\overline{\Theta})^\alpha\} \{(\underline{d})^{1-\alpha}(\overline{d})^\alpha + (\underline{\epsilon})^{1-\alpha}(\overline{\epsilon})^\alpha + (\underline{\varphi})^{1-\alpha}(\overline{\varphi})^\alpha\}}$$

and $R_{0f} = \frac{D_f(\tilde{\lambda})D_f(\tilde{\theta})D_f(\tilde{B})}{D_f(\tilde{d})(D_f(\tilde{d}) + D_f(\tilde{\theta}))(D_f(\tilde{d}) + D_f(\tilde{\epsilon}) + D_f(\tilde{\varphi}))}$

4.3 Equilibria

The SEIRUS model has two biologically equilibrium points. They are namely

- (i) infection free steady state $E_0(S_0, E_0, I_0, R_0, U_0) = (\frac{B}{d}, 0, 0, 0, 0)$ and
- (ii) endemic equilibrium point $E^*(S^*, E^*, I^*, R^*, U^*)$, where

$$S^* = \frac{(d+\theta)(d+\epsilon+\varphi)}{\lambda\Theta}, E^* = \frac{(d+\epsilon+\varphi)I^*}{\theta},$$

$$I^* = \frac{[B\lambda\Theta - d(d+\theta)(d+\epsilon+\varphi)][(d+\mu+\gamma)(d+\sigma)]}{\lambda(d+\theta)(d+\epsilon+\varphi)(d+\sigma)(d+\mu+\gamma) - \lambda\Theta\sigma\mu},$$

$$R^* = \frac{\epsilon I^*}{d+\mu+\gamma}, U^* = \frac{\mu \epsilon I^*}{(d+\mu+\gamma)(d+\sigma)}$$

Theorem 5: If $R_0 < 1$ ($R_0 > 1$) with the condition $\lambda\Theta < d(d + \theta)(d + \epsilon + \varphi)$, the equilibrium E_0 in disease free condition, is locally asymptotically stable (unstable).

Proof: At the disease free equilibrium point $E_0 = (S_0, 0, 0, 0, 0)$, the characteristic equation of the system (1) is given by

$$(x + d)[x^2 + (2d + \Theta + \epsilon + \varphi)x + (d + \Theta)(d + \epsilon + \varphi) - \lambda\Theta S_0](x + d + \mu + \gamma)(x + d + \sigma) = 0$$

All roots becomes negative if the following condition holds

- (i) $2d + \theta + \epsilon + \varphi > 0$
- (ii) $d(d + \theta)(d + \epsilon + \varphi) - \lambda\Theta B > 0$

$$\text{i.e. } R_0 = \frac{\lambda\Theta B}{d(d+\theta)(d+\epsilon+\varphi)} < 1$$

$$\text{or } \lambda\Theta B < d(d + \theta)(d + \epsilon + \varphi)$$

Hence the system (1) will be locally asymptotically stable at disease free equilibrium point for $R_0 < 1$ with $\lambda\Theta < d(d + \theta)(d + \epsilon + \varphi)$ and it is unstable for $R_0 > 1$.

Therefore the theorem is proved.

In similar way we have written the theorem.

Theorem 6: If $R_{0h} < 1$ ($R_{0h} > 1$) with the condition $(\underline{\lambda})^{(1-\alpha)}(\overline{\lambda})^\alpha(\underline{\Theta})^{(1-\alpha)}(\overline{\Theta})^\alpha(\underline{B})^{(1-\alpha)}(\overline{B})^\alpha$

where, $M_1 = 5d + \Theta + \epsilon + \varphi + \lambda I^* + \mu + \gamma + \sigma$

$$M_2 = 2d(\lambda I^* + \mu + \gamma + \sigma + 3d + 2\epsilon + 2\varphi + 2\theta) + \theta(\lambda I^* + \mu + \gamma + \sigma + \epsilon + \varphi)$$

$< (\underline{d})^{(1-\alpha)}(\overline{d})^\alpha \{(\underline{d})^{(1-\alpha)}(\overline{d})^\alpha + (\underline{\Theta})^{(1-\alpha)}(\overline{\Theta})^\alpha\} \{(\underline{d})^{(1-\alpha)}(\overline{d})^\alpha + (\underline{\epsilon})^{(1-\alpha)}(\overline{\epsilon})^\alpha + (\underline{\varphi})^{(1-\alpha)}(\overline{\varphi})^\alpha\}$, the disease free equilibrium E_0 is locally asymptotically stable (unstable).

Theorem 7: If $R_{0f} < 1$ ($R_{0f} > 1$) with the condition $D_f(\tilde{\lambda})D_f(\tilde{\theta})D_f(\tilde{B}) < D_f(\tilde{d})(D_f(\tilde{d}) + D_f(\tilde{\theta}))(D_f(\tilde{d}) + D_f(\tilde{\epsilon}) + D_f(\tilde{\varphi}))$, the disease free equilibrium E_0 is locally asymptotically stable (unstable).

Theorem 8: Let us assume that all of M_1, N_2, N_3, N_4 are positive. Then the crisp model (1) is locally asymptotically stable around its endemic equilibrium point.

Proof: The characteristic equation of the system (1) at point E_1^* is constructed as

$$x^5 + M_1x^4 + M_2x^3 + M_3x^2 + M_4x + M_5 = 0$$

$$+ \epsilon(\mu + \gamma + \tilde{\sigma}) + \varphi(\lambda I^* + \mu + \gamma + \sigma) + \lambda\Theta S^*$$

$$\begin{aligned}
 M_3 &= \lambda\Theta S^*(2\lambda I^* + \mu + \gamma + \sigma + 3d) + \lambda I^*[d(\Theta + \epsilon + \varphi + 2\sigma + 2\mu + 2\gamma) \\
 &\quad + \Theta(\epsilon + \varphi) + 2\sigma(\mu + \gamma)] + (\mu + \gamma + \sigma + 3d)(\Theta\epsilon + \Theta\varphi + d\epsilon + d\varphi + d\Theta) \\
 &\quad + d(d + \sigma d + \mu d + \gamma d + \gamma\sigma) \\
 M_4 &= [\lambda\Theta S^* + d(\Theta + \epsilon + \varphi) + \Theta(\epsilon + \varphi)][\lambda I^*(\mu + \gamma + \sigma + 2d) + d(3d + 2\mu + 2\gamma) + \sigma(\mu + \gamma)] \\
 &\quad + \lambda I^*(\sigma d + \mu d + \gamma d + \mu\sigma + \gamma\sigma) + d(\sigma d + \mu d + \gamma d + \mu\sigma + \gamma\sigma + d^2)(2d + \Theta + \epsilon + \varphi) \\
 M_5 &= [\lambda\Theta S^* + d(\Theta + \epsilon + \varphi) + \Theta(\epsilon + \varphi)][\lambda I^* + (\sigma d + \mu d + \gamma d + \mu\sigma + \gamma\sigma) \\
 &\quad + d(d^2 + \sigma d + \mu d + \gamma d + \mu\sigma + \gamma\sigma)] - \lambda\Theta\sigma\epsilon\mu I^*
 \end{aligned}$$

Let us assume $N_1 = M_1$, $N_2 = M_1M_2 - M_3$, $N_3 = M_1M_2M_3 - M_3^2 - M_1^2M_4 + M_1M_5$, $N_4 = M_1M_2M_3M_4 - M_3^2M_4 - M_1^2M_4 - M_1M_2^2M_5 + M_2M_3M_5 + 2M_1M_4M_5 - M_5^2$.

Assuming that all $M_1, M_3, M_4, M_5, N_2, N_3$ and N_4 are positive. We apply the Routh-Hurwitz criteria. Then the system (1) is locally asymptotically stable around E_1^* .

Hence theorem is proved.

Theorem 9: If $B \leq K_{\max}$ then the crisp model system (1) is globally asymptotically stable around its endemic equilibrium point E_1^* .

Proof: Let us assume the Lyapunov function $Z(t)$ in the following way

$$Z = S + E + I + R + U$$

Both side taking time derivative of Z , we get

$$\frac{dZ}{dt} = B - d(S + E + I + R + U) - \varphi I - \gamma R$$

Now let us assume that $K_{\max} = d(S_{\max} + E_{\max} + I_{\max} + R_{\max} + U_{\max}) + \varphi I_{\max} + \gamma R_{\max}$ where, I_{\max} and R_{\max} are the largest value of I, R respectively. We provide all the largest values are finite. If $B \leq K_{\max}$ then $\frac{dZ}{dt} \leq 0$ although $Z(t) \geq 0$.

Hence, we have concluded that the system (1) is global stability around its endemic equilibrium point.

Thus theorem is proved.

Similar manners hold for interval type model and fuzzy model.

5. Optimality of System

In this portion, we describe the optimal control problem to observe how proper control policy diminishes the disease from the population. In COVID-19 disease people mainly infected when they come into the infected people both asymptomatic and symptomatic people. So the precautionary measure maintaining social distance, using face mask in mass gathering area are the important factor to diminish the disease fatality. We take the incurred cost that needs to minimize by

applying control interventions. With the help of Pontryagin's Maximum principle [54], we form the objective functional

$$L_1 = \min_{v_1, v_2} \int_0^{T_1} (k_1 I + k_2 v_1^2 + k_3 v_2^2) dt$$

Subject to the system

$$\frac{dS(t)}{dt} = B - (1 - v_1)\lambda SI - dS + \sigma U - v_2 S$$

$$\frac{dE(t)}{dt} = (1 - v_1)\lambda SI - dE - \Theta E$$

$$\frac{dI(t)}{dt} = \Theta E - (d + \epsilon + \varphi) I$$

$$\frac{dR(t)}{dt} = \epsilon I - (d + \mu + \gamma) R$$

$$\frac{dU(t)}{dt} = v_2 S + \mu R - (d + \sigma) U \tag{5}$$

where, $S(0), E(0), I(0), R(0), U(0)$ are all positive. We assume that k_1 is the per capita loss due to presence of infected population at any time. The square of control parameter is chosen to remove the severity of side effect [52, 53]. v_1 is considered precautionary measure (like maintain social distance, using face mask in mass gathering) and v_2 is considered due to protective measure (like maintaining suitable hygiene, staying in isolation) susceptible population directly moves to recovered population. k_2 and k_3 are the weighted function of v_1 and v_2 respectively. Assuming k_1, k_2, k_3 are positive constant in time interval $[0, T_1]$. The main theme of our work is to determine optimal response intensity and optimal treatment with minimum cost. So the area of the control intervention $v_1(t), v_2(t)$ is given as follows:

$$\begin{aligned}
 \Psi &= \{(v_1(t), v_2(t)) : (v_1(t), v_2(t)) \\
 &\quad \in [0, 1] \times [0, 1], t \in [0, T_1]\}
 \end{aligned}$$

where $v_1(t), v_2(t)$ are measurable and bounded function for $t \in [0, T_1]$. When people take a full violation of precautionary measure (like social distance) then $v_1(t)$ takes lowest value which

is 0. When people takes full maintaining the pre-cautionary measure then $v_1(t)$ takes highest value which is 1. In other situation the control variable is in $v_1(t) \in (0, 1)$. $v_2(t)$ represents as control policy which is due to protective measure susceptible population directly moves to recovered population. From beginning it satisfies $0 \leq v_2(t) \leq 1$.

Theorem 10: In the region $\psi = \{(v_1(t), v_2(t)) : (v_1(t), v_2(t)) \in [0, 1] \times [0, 1], t \in [0, T_1]\}$ the optimal control intervention (v_1^*, v_2^*) which minimizes L_1 is given by $v_1^* = \max\{0, \min(\bar{v}_1, 1)\}$ and $v_2^* = \max\{0, \min(\bar{v}_2, 1)\}$ where $\bar{v}_1 = \frac{(\tau_2 - \tau_1)\lambda SI}{2k_2}$, $\bar{v}_2 = \frac{(\tau_1 - \tau_5)S}{2k_3}$.

Proof: The Lagrangian of the problem is given by

$$L_2 = k_1 I + k_2 v_1^2 + k_3 v_2^2.$$

Let us define the Hamiltonian function as

$$\begin{aligned} \bar{H}(S, E, I, R, U, v_1, v_2, \tau) \\ = L_2(I, v_1, v_2) + \tau_1 \frac{dS}{dt} + \tau_2 \frac{dE}{dt} + \tau_3 \frac{dI}{dt} \\ + \tau_4 \frac{dR}{dt} + \tau_5 \frac{dU}{dt}. \end{aligned}$$

Here $\tau = (\tau_1, \tau_2, \tau_3, \tau_4, \tau_5)$ are adjoint variable. Using Pontryagin's maximum principle we get minimized Hamiltonian to minimize the cost functional. The Hamiltonian can be determined by solving the following differential equations

$$\begin{aligned} \frac{d\tau_1}{dt} = -\frac{\partial \bar{H}}{\partial S} = \tau_1 \{(1 - v_1)\lambda I + d + v_2\} \\ - \tau_2 \{(1 - v_1)\lambda I\} - \tau_5 v_2 \end{aligned}$$

Table 1: Input Data of the Crisp Model

Parameters	Values (Disease free equilibrium)	Data Source	Values (Endemic equilibrium)	Data Source
B	0.00567 per day	Assumed	0.00567 per day	Assumed
λ	10^{-6} /person/day	Assumed	10^{-6} /person/day	Assumed
d	10^{-3} /person/day	Victor [48]	10^{-3} /person/day	Victor [48]
σ	0.28404/day	Nesteruk [36]	0.28404/day	Nesteruk [36]
Θ	0.27 per day	Assumed	0.1 per day	Assumed
ϵ	0.095 per day	Assumed	0.095 per day	Assumed
φ	0.005 per day	Assumed	0.005 per day	Assumed
μ	0.1 per day	JHH [20]	0.1 per day	JHH [20]
γ	6×10^{-7} per day	Assumed	6×10^{-7} per day	Assumed
T	14 day	WHO (2020) [18]	14 day	WHO (2020) [18]

$$\begin{aligned} \frac{d\tau_2}{dt} &= -\frac{\partial \bar{H}}{\partial E} = (d + \Theta)\tau_2 - \tau_3 \Theta \\ \frac{d\tau_3}{dt} &= -\frac{\partial \bar{H}}{\partial I} = -k_1 + \tau_1(1 - v_1)\lambda S \\ &\quad - \tau_2(1 - v_1)\lambda S + \tau_3(d + \epsilon + \varphi) - \tau_4 \epsilon \\ \frac{d\tau_4}{dt} &= -\frac{\partial \bar{H}}{\partial R} = \tau_4(d + \mu + \gamma) - \tau_5 \mu \\ \frac{d\tau_5}{dt} &= -\frac{\partial \bar{H}}{\partial U} = -\tau_1 \sigma + \tau_5(d + \sigma) \end{aligned} \tag{6}$$

Satisfying the transversality condition $\tau_i(T_1) = 0$, $i = 1, 2, 3, 4, 5$. From optimality conditions: $\frac{\partial \bar{H}}{\partial v_1} = 0$ and $\frac{\partial \bar{H}}{\partial v_2} = 0$ at the point $v_1 = \bar{v}_1$ and $v_2 = \bar{v}_2$ respectively. We have

$$v_1 = \bar{v}_1 = \frac{(\tau_2 - \tau_1)\lambda SI}{2k_2} \text{ and } v_2 = \bar{v}_2 = \frac{(\tau_1 - \tau_5)S}{2k_3}.$$

The lower bound and upper bound of two controls are 0 and 1 respectively. Therefore, we have $v_1^* = 0$ if $\bar{v}_1 < 0$ and $v_1^* = 1$ if $\bar{v}_1 > 1$, otherwise $v_1^* = \bar{v}_1$. Similar results hold for other control parameter v_2 . Hence, the theorem is proved.

6. Numerical Results

The systems of equations are solved by MATLAB packages. We use the parameters in the embodiment of the model are given below in the Table 1. We choose the parameter value in consensus with the suitable value for obtaining the stability of the disease free equilibrium state of the model and also we have managed supposition data for this work.

Result 1. Crisp Model

We take the crisp values of the parameter from the **Table 1**. **Fig. 2** presents the solution curves for disease free equilibrium. We see that susceptible population is increase as time increases. From the figure, we conclude that the system has only the disease free equilibrium and it is locally asymptotically stable (see **Fig. 3**), i.e., exposed, infected, quarantined or isolated and recovered population are extinct from the system. This is happened because rate of spreading infection to the contact with exposed populations (λ) and force of infection rate (Θ) is small. For the higher values of θ , there exists endemic equilibrium for the system (1). Now, if we take the value $\Theta = 0.1$ and other

parameter values are unchanged i.e. we take the values (Endemic equilibrium) from **Table 1**, we can get the solution curves for endemic equilibrium. From **Fig. 3** we see that exposed, infected, quarantined or isolated and recovered populations are in decreasing order after 100 days (approx). We have drawn the phase space trajectories for different classes of population in **Fig. 4** with the help of same set of parametric values (**Table 1**). In this figure exposed population, infected population, quarantined or isolated population and recovered population are plotted with respect to susceptible population. Also we have plotted recovered population with respect to infected population and quarantined or isolated population.

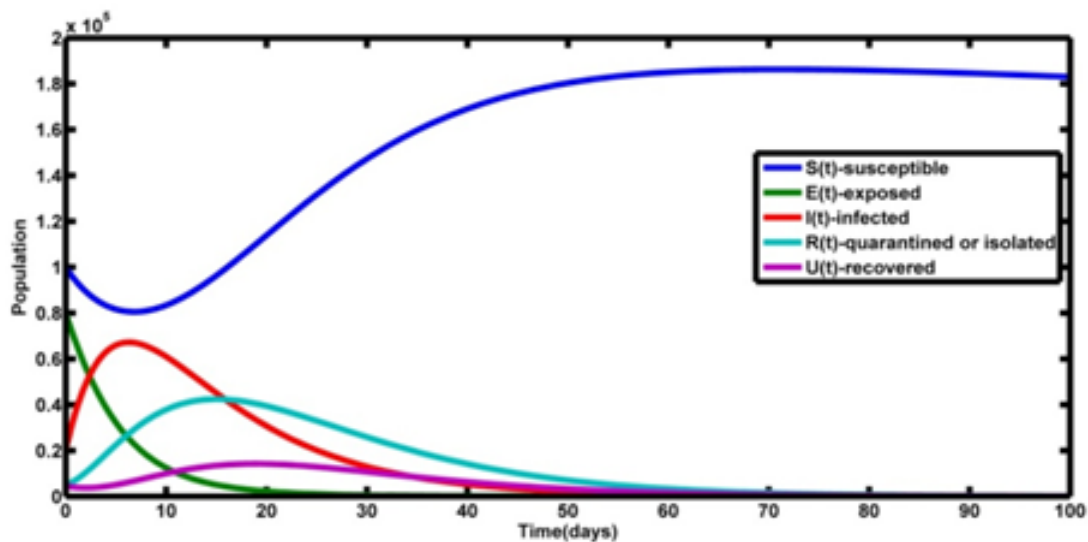


Fig. 2. Solution curves of disease free equilibrium point

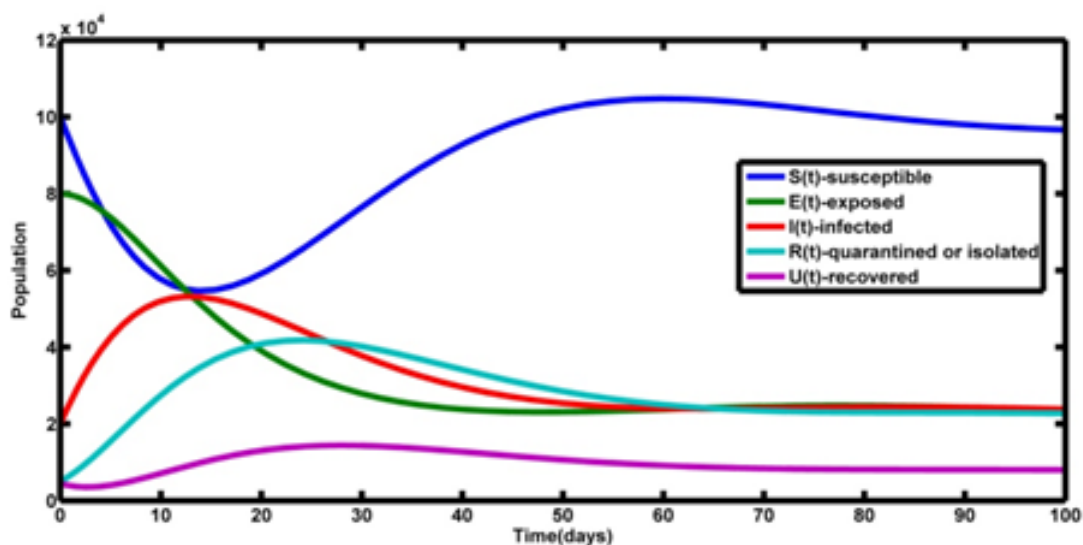


Fig. 3. Solution curves of endemic equilibrium point

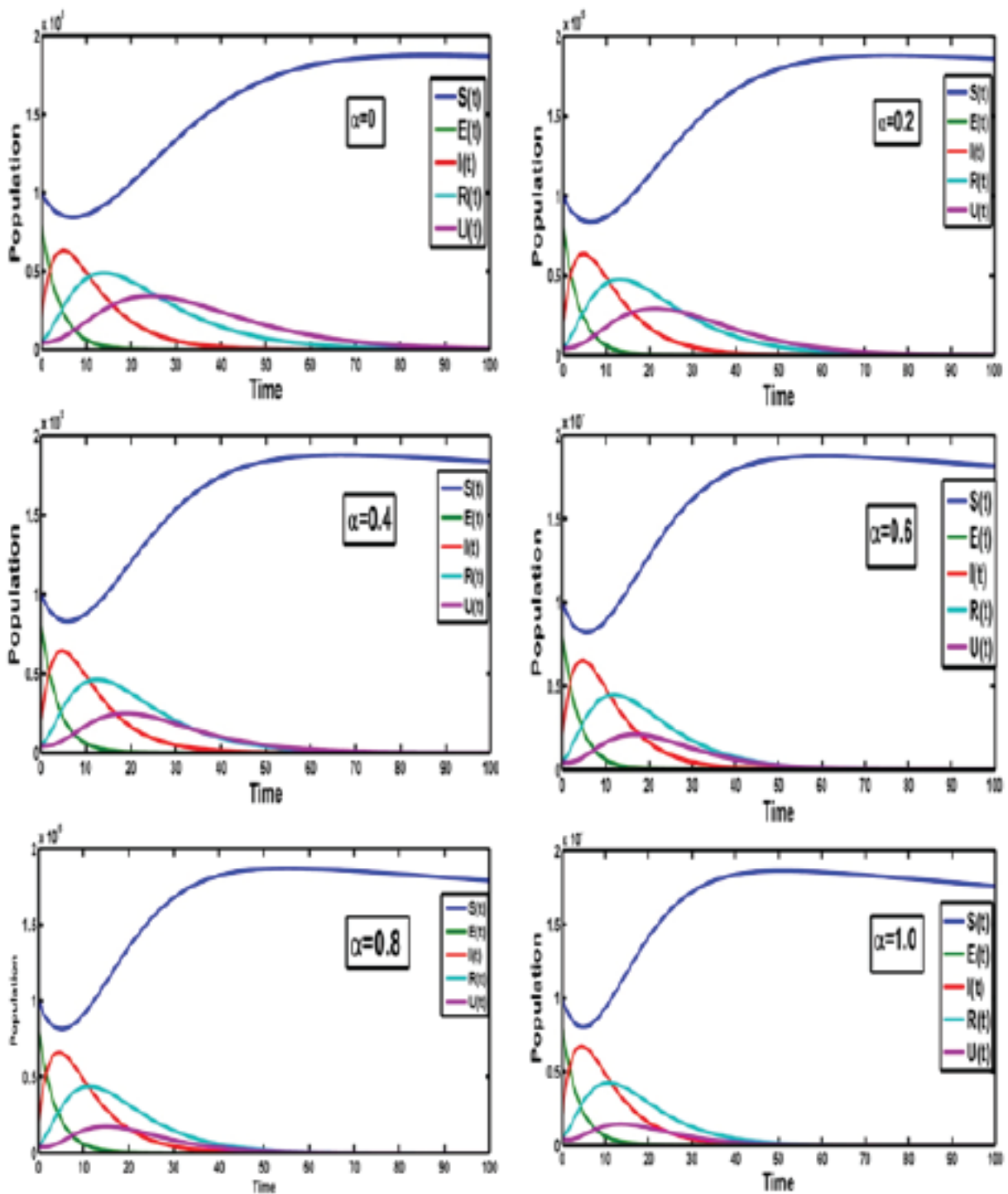


Fig. 4. Solution curves of the disease free equilibrium point in different values of α

Result 2: Interval SEIRUS Model

In this portion, we set the values of the parameters as interval numbers given in Table 2. Fig. 4 and Fig. 5 represent the solution curve of the system (2) for disease free equilibrium and endemic equilibrium for the different values of α . In Fig. 4 we see that the susceptible populations are increasing

as time increase for the different values of α . In Fig. 5 we observe that exposed, infected, quarantined or isolated, recovered population decrease after 40–60 days and the susceptible population increase slightly as time increase for the different values of α .

Table 2: Input Data of the Interval Model

Interval Valued Parameters	Interval Values (Disease Free Equilibrium)	Interval Values (Endemic Equilibrium)
$[\underline{B}, \overline{B}]$	$[4.536 \times 10^{-3}, 7.938 \times 10^{-3}]$	$[4.536 \times 10^{-3}, 7.938 \times 10^{-3}]$
$[\underline{\lambda}, \overline{\lambda}]$	$[8 \times 10^{-7}, 1.4 \times 10^{-6}]$	$[8 \times 10^{-7}, 1.4 \times 10^{-6}]$
$[\underline{d}, \overline{d}]$	$[8 \times 10^{-4}, 1.4 \times 10^{-3}]$	$[8 \times 10^{-4}, 1.4 \times 10^{-3}]$
$[\underline{\sigma}, \overline{\sigma}]$	$[0.08521, 0.3976]$	$[0.08521, 0.3976]$
$[\underline{\epsilon}, \overline{\epsilon}]$	$[0.076, 0.133]$	$[0.114, 0.133]$
$[\underline{\mu}, \overline{\mu}]$	$[0.08, 0.14]$	$[0.08, 0.14]$
$[\underline{\Theta}, \overline{\Theta}]$	$[0.216, 0.378]$	$[0.08, 0.14]$
$[\underline{\varphi}, \overline{\varphi}]$	$[4 \times 10^{-3}, 7 \times 10^{-3}]$	$[4 \times 10^{-3}, 7 \times 10^{-3}]$
$[\underline{\gamma}, \overline{\gamma}]$	$[4 \times 10^{-7}, 8.4 \times 10^{-7}]$	$[4 \times 10^{-7}, 8.4 \times 10^{-7}]$

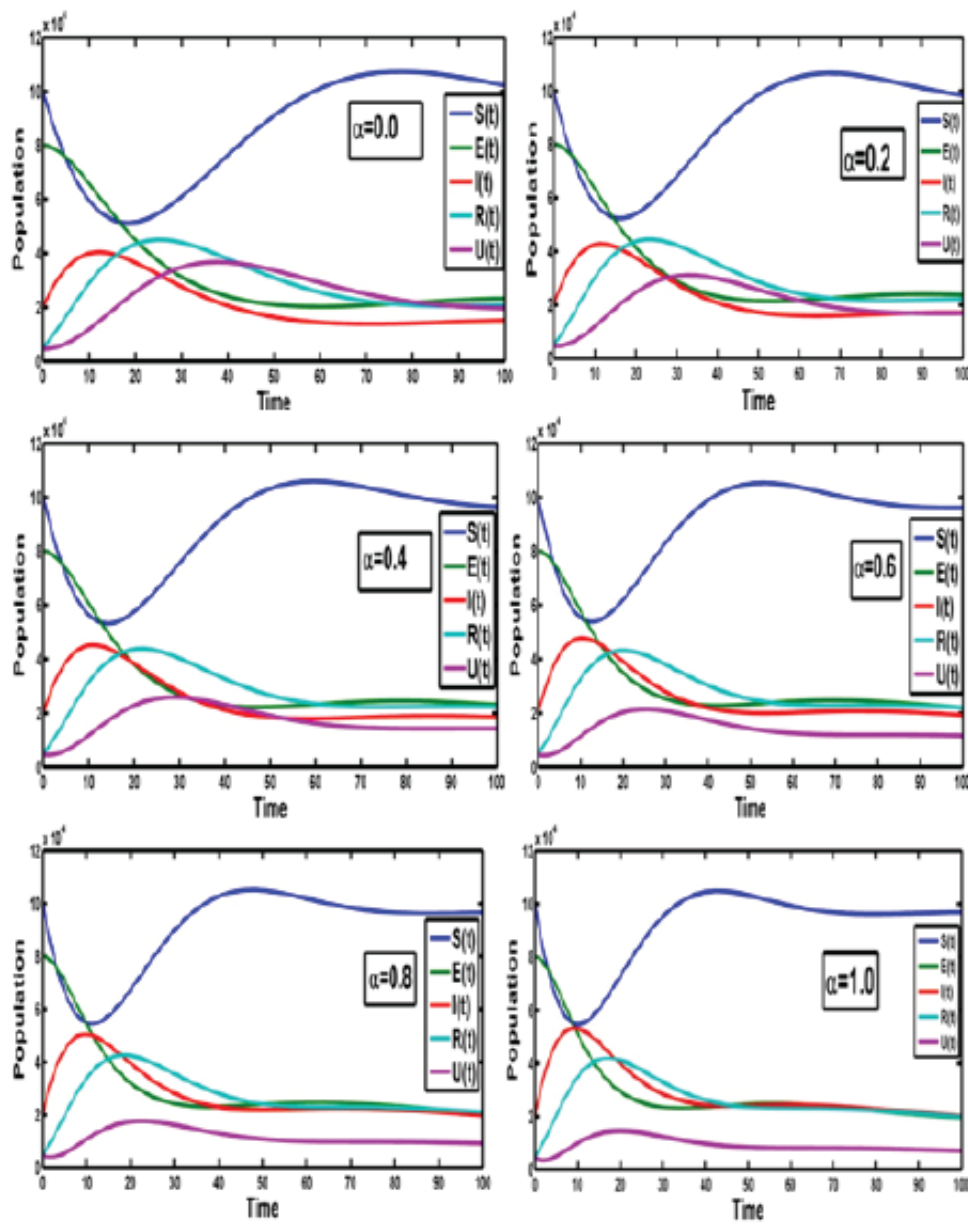


Fig. 5. Solution curves at the endemic equilibrium point for different values α

Result 3: Fuzzy SEIRUS Model

We take all the parameters as triangular fuzzy number. We defuzzified the values of the parameter by using Graded mean integration value technique. The variation graphs for different values of q are represented. **Fig. 6** presents the variation of susceptible, exposed, infected, quarantined or isolated and recovered populations

for the different values of q in fuzzy environment. Here, dark blue, pink, green, yellow, red lines indicate the populations at $q = 0, q = 0.2, q = 0.5, q = 0.7, q = 1$ respectively. It is observed that a slight deflection can be arisen on the population curves. All the curves will meet at one stage. This implies that the solution point will be same for some values of time t .

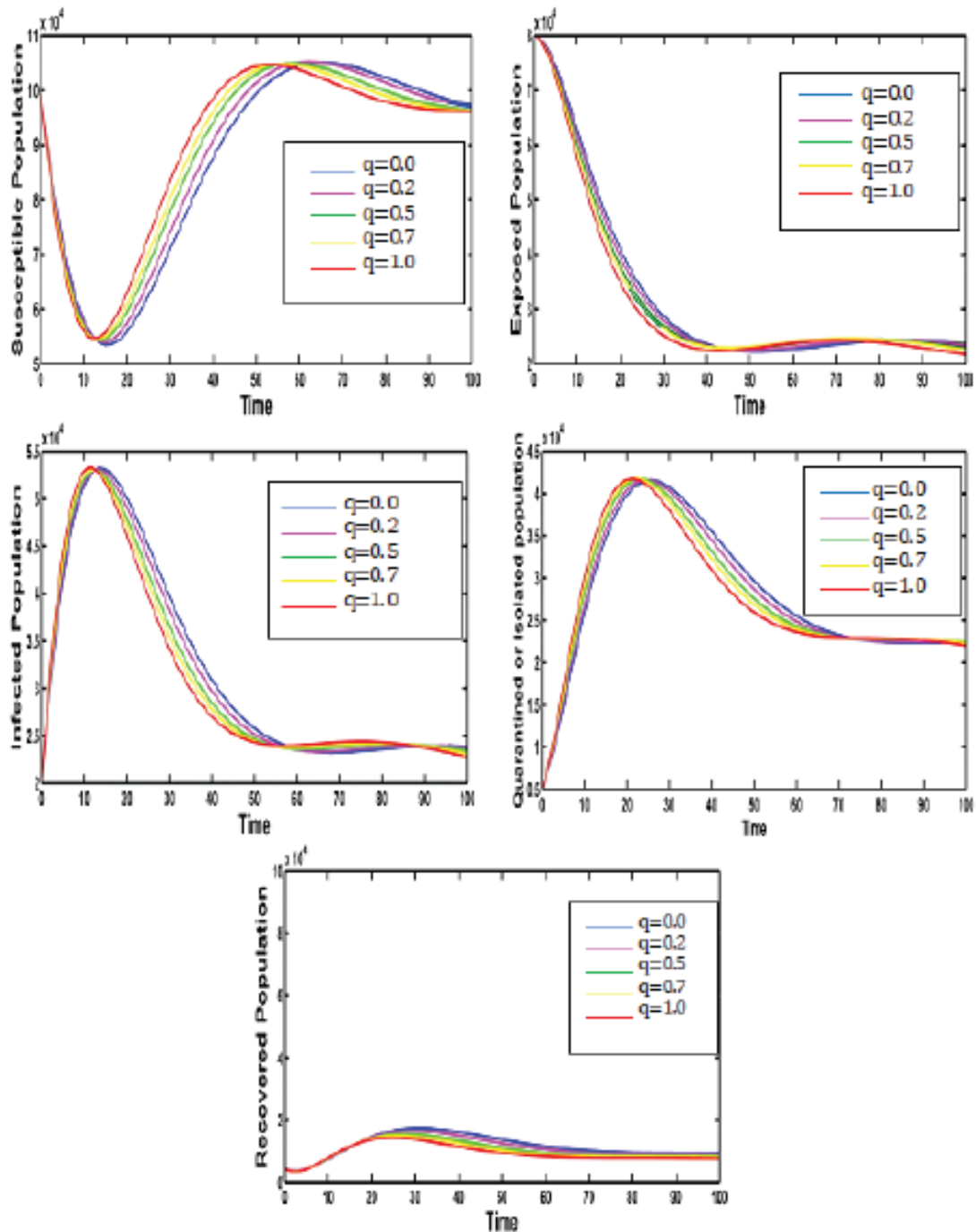


Fig. 6. Variation of populations at endemic equilibrium for different values of q

Table 3: Input Data of the Fuzzy Model

Parameters	TFN
\tilde{B}	$(4.53 \times 10^{-3}, 0.00567, 7.93 \times 10^{-3})$
$\tilde{\lambda}$	$(8 \times 10^{-7}, 10^{-6}, 1.4 \times 10^{-6})$
\tilde{d}	$(8 \times 10^{-4}, 10^{-3}, 1.4 \times 10^{-3})$
$\tilde{\sigma}$	$(0.0852, 0.28404, 0.3976)$
$\tilde{\epsilon}$	$(0.076, 0.095, 0.133)$
$\tilde{\mu}$	$(0.08, 0.1, 0.14)$
$\tilde{\Theta}$	$(0.08, 0.1, 0.14)$
$\tilde{\varphi}$	$(4 \times 10^{-3}, 0.005, 7 \times 10^{-3})$
$\tilde{\gamma}$	$(4.8 \times 10^{-7}, 6 \times 10^{-7}, 8.4 \times 10^{-7})$

7. Sensitivities of Parameters of the Crisp Model

In this section, we have described the sensitivities of parameters of the crisp model (1). We have investigated the sensitivity analysis of the system (1) with respect to the parameter disease transmission rate from exposed population to susceptible population (λ), proportion of observed population and being moved to susceptible population (σ), force of infection rate of the population (Θ), rate of recovery of quarantined or isolated population (μ).

Sensitivity of λ : We see that the numbers of exposed, infected, quarantined or isolated and

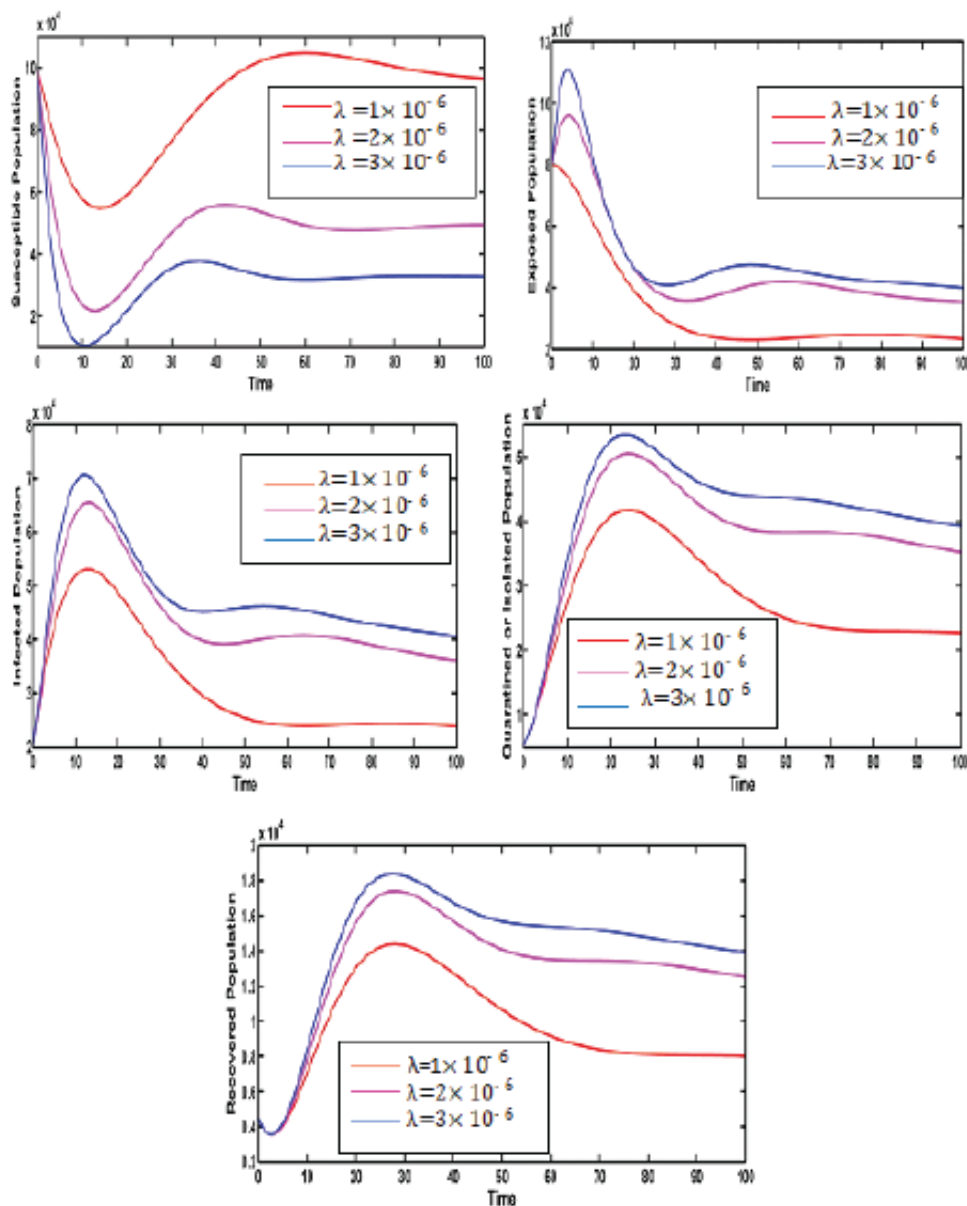


Fig. 7. Sensitivity of the system (1) for different values λ

recovered populations are directly proportional with disease transmission rate. i.e. if disease transmission rate is increased then exposed, infected, quarantined and recovered populations are also increased. But for the susceptible population we have observed reverse scenario. All the populations are influenced by varying the parameter λ . **Fig. 7** illustrates the sensitivity of different value of λ .

Sensitivity of the parameter Θ : In the sensitivity of the parameter Θ , we see that susceptible population is directly proportional to the parameter force of infection rate. But reverse scenario can be shown for the exposed population. The infected population and quarantine or isolated population are increased firstly as the value of Θ is increased. **Fig. 8** represents the sensitivity of Θ .

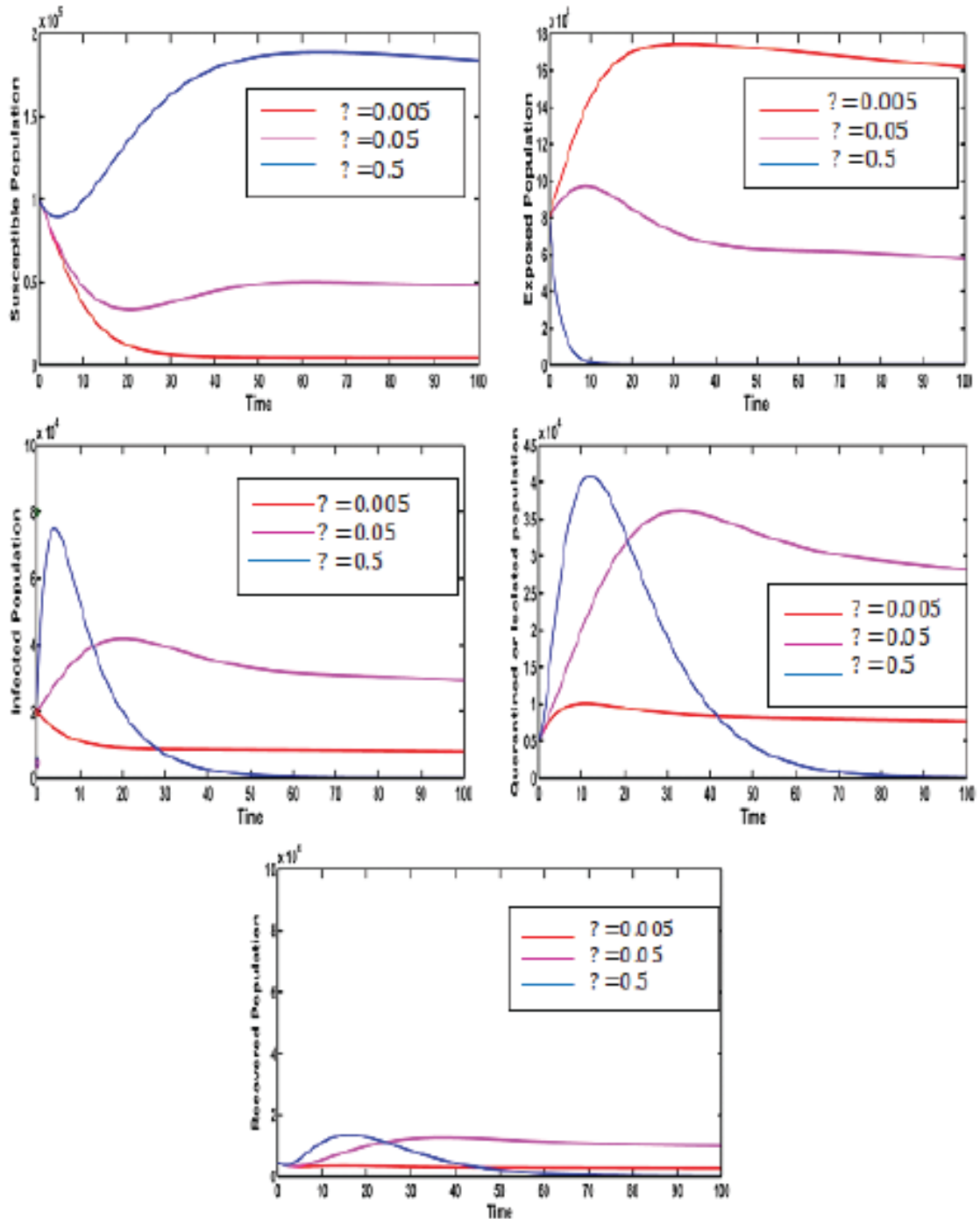


Fig. 8. Sensitivity of the system (1) for different values of θ

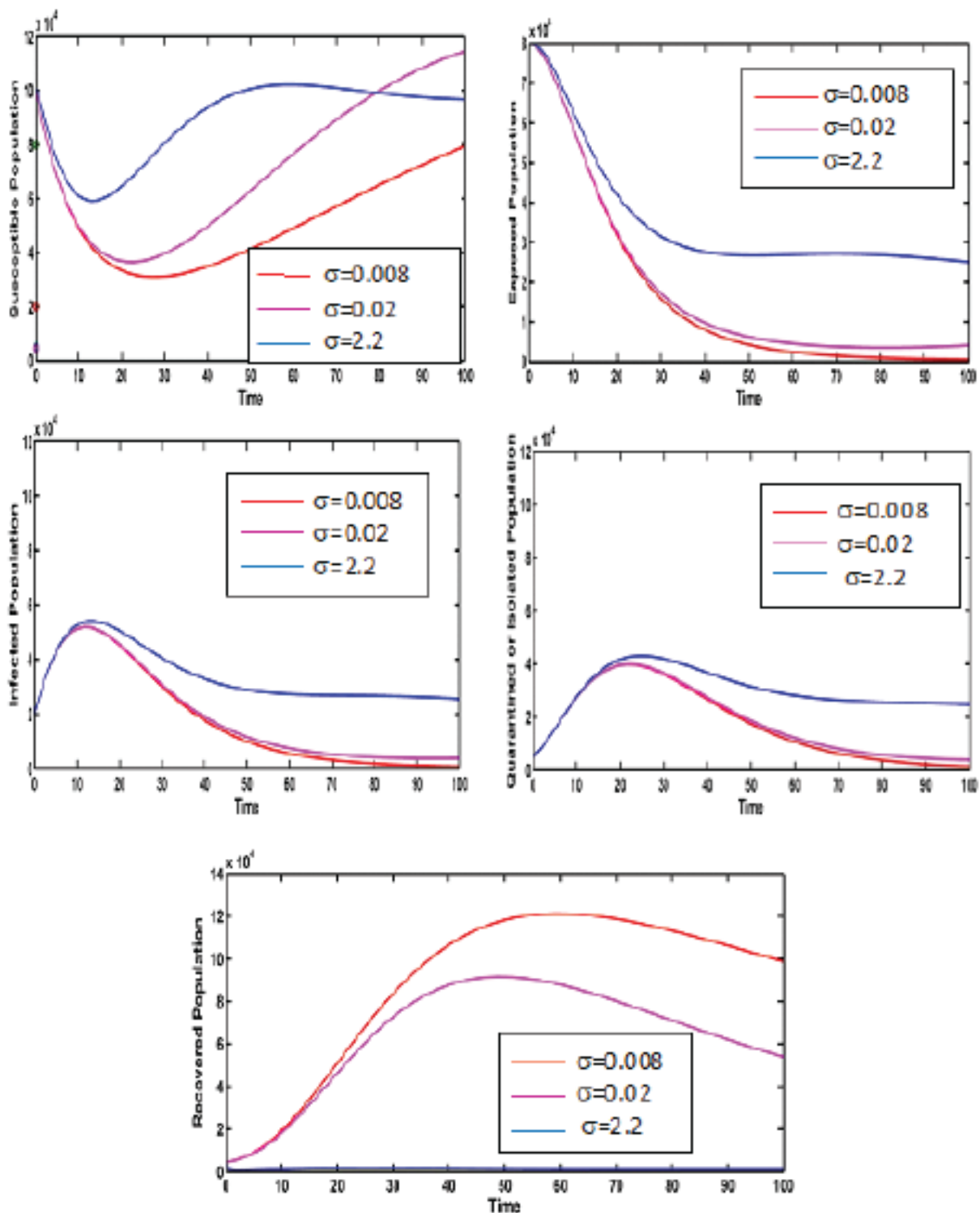


Fig. 9. Sensitivity of the system (1) for different values of σ

Sensitivity of the parameter σ : In the sensitivity of σ we see that susceptible population is directly proportional to σ , observed population moved to susceptible but reverse scenario can be presented for the recovered population. Infected,

quarantined or isolated population are gradually increased with the increase of the value σ . Fig. 9 indicates the sensitivity of σ .

Sensitivity of the parameter μ : In the sensitivity of μ we have observed that susceptible,

exposed, infected, recovered population are directly proportional to μ recovery rate of quarantined or isolated population. But quarantine or

isolated population are inversely proportion to μ . We have drawn **Fig. 10** for sensitivities of the different values of μ .

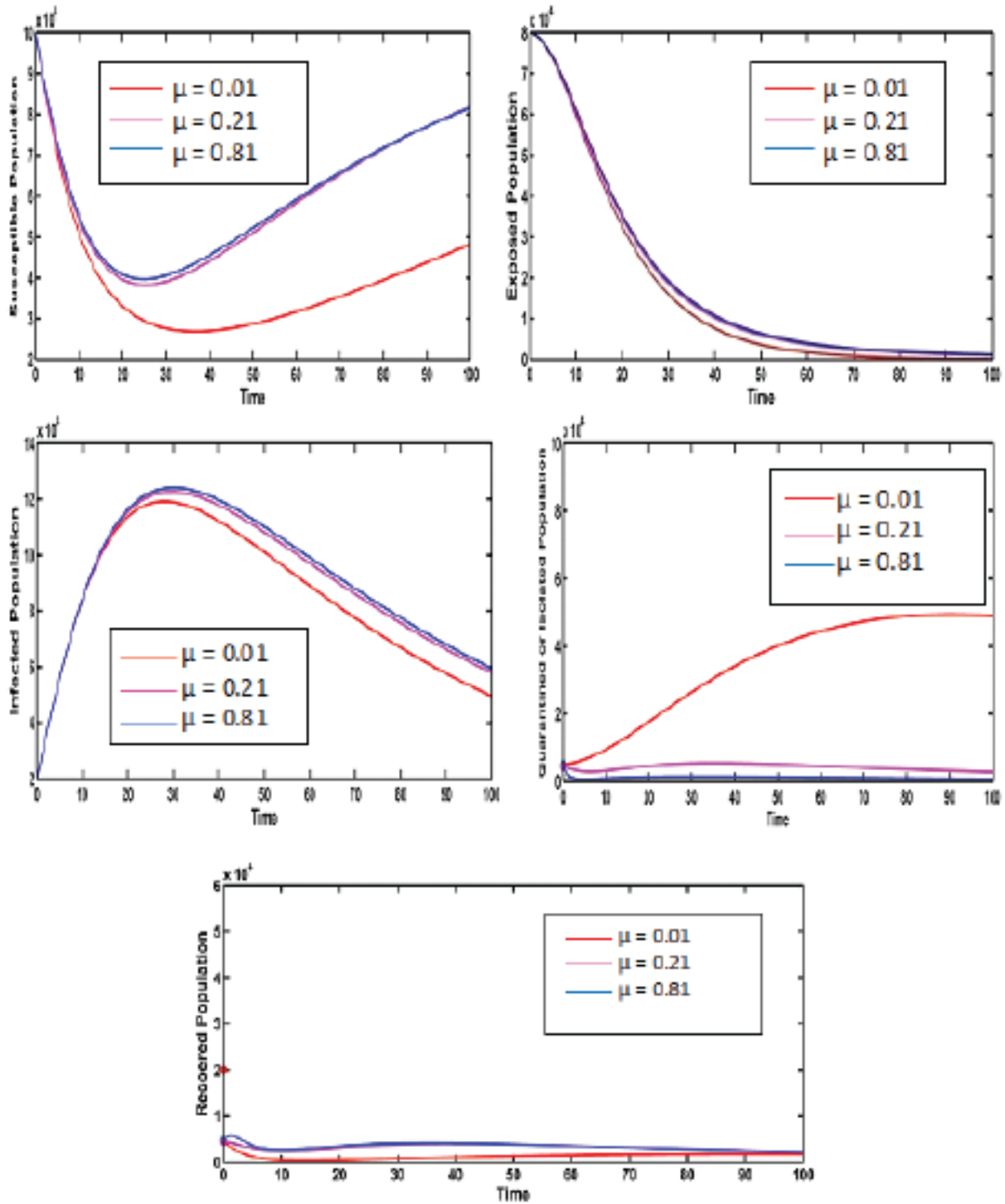


Fig. 10. Sensitivity of the different value of μ

8. Numerical Results with Control Policies

We have found the optimal control variables with the help of forward-backward sweep method. We have solved the optimal state system and adjoint state system using forward and backward in time respectively. Assuming the control policies are implemented for $T_1 = 100$ days. We have used the set of parameters like $B = 0.00567$, $\lambda = 10^{-6}$, $d = 10^3$, $\sigma = 0.28404$, $\Theta = 0.1$, $\epsilon = 0.095$, $\varphi = .005$, $\mu = 0.1$, $\gamma = 6 \times 10^{-7}$, $k_1 = 1$, $k_2 = 100$, $k_3 = 100$ and considered the initial values of the state variables as $S(0) = 500000$, $E(0) = 1000$,

$I(0) = 475$, $R(0) = 100$, $U(0) = 90$. We have represented the figures for the optimal control problem using MATLAB. **Fig. 11** represents the population trajectories for both control policies. From the **Fig. 11** it is observed that the susceptible population increase with time. When the people maintain social distance and take precautionary measure for the infectious disease then the infected population and quarantined or isolated population decreases gradually. Also the count of recovered individuals increases significantly. The variations of adjoint or costate variables are represented in **Fig. 12**.

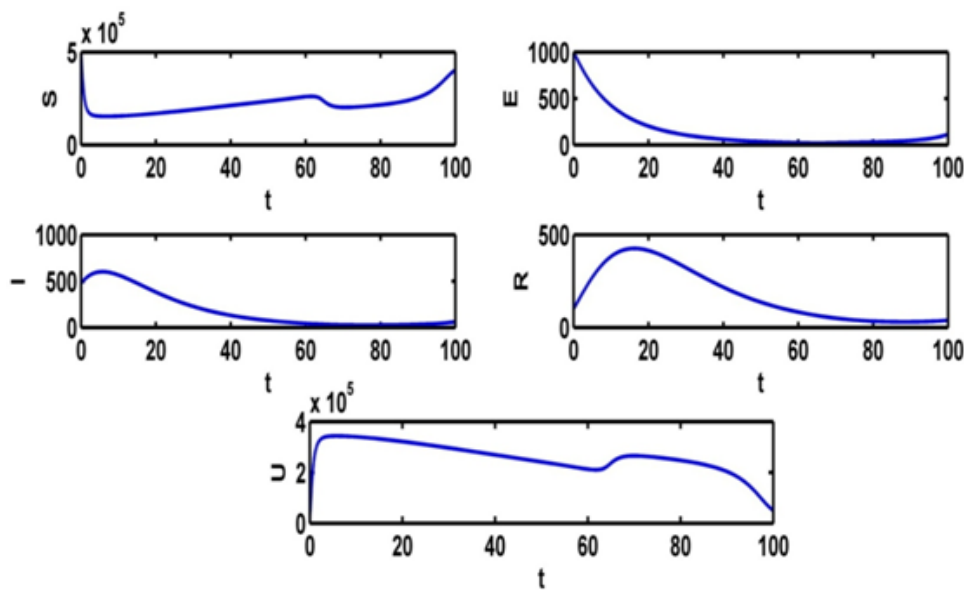


Fig. 11. Profiles of populations with applied optimal control v_1^* and v_2^*

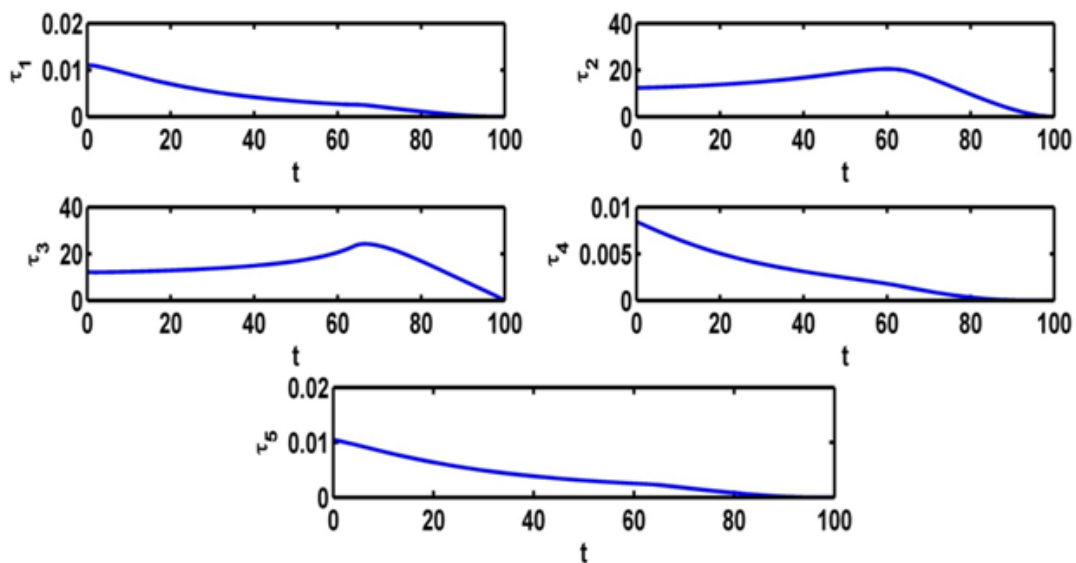


Fig. 12. Variation of adjoint variables as time evolves

Fig. 13 represents the path of optimal control policies v_1^* , v_2^* . People maintain social distance and take precautionary measure, and then the

virus cannot be transmitted in the population which indicates that control strategy works with higher intensity over the time period.

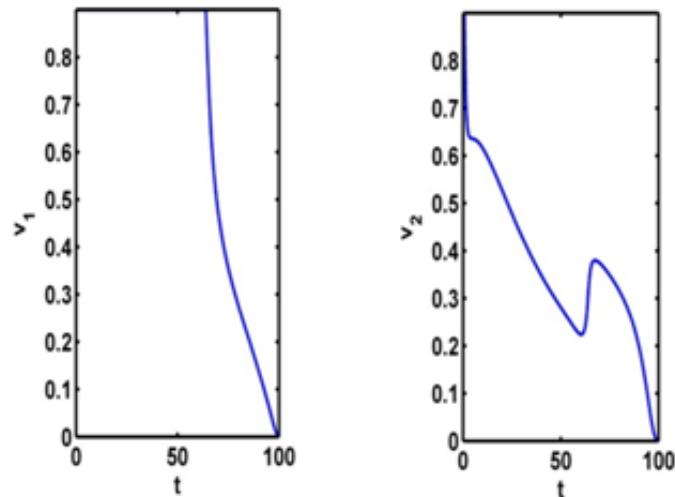


Fig. 13. Profile of control parameters as time evolves

9. Conclusions

In this work, we developed the COVID-19 SEIRUS model which is quite different from other traditional epidemic models. In the theoretical portion, the boundedness of the system is studied. Also, the disease free equilibrium and endemic equilibrium are investigated. Further, the condition of stability of the system and the condition for locally asymptotically stability are investigated and basic reproduction number is also computed. Also, the COVID-19 SEIRUS model is converted to the fuzzy SEIRUS model and the interval SEIRUS model. Solution curves are drawn for both disease free equilibrium and endemic equilibrium in **Fig. 2** and **Fig. 3** respectively. With respect to different population the phase space trajectories of the crisp SEIRUS model are illustrated in **Fig. 4**. For fuzzy SEIRUS model, we have drawn variation of populations at endemic equilibrium for different values of q in **Fig. 6**. We have explained the sensitivity of the controlled parameter λ , Θ , σ and μ . When the force of infection rate (Θ) is low then the basic reproduction number must be less than 1 and when infection rate increases then basic reproduction number is greater than 1. From the sensitivity of the parameter, we see that when the people are in quarantine or isolation the rate of infection decreased. It is concluded that all the population is significantly influenced by the impreciseness of parameters. Therefore, the fuzzy model is more robust

than crisp ones. The findings in this study also indicate that we should be prepared to fight the corona virus disease for a much longer term than that of the current epidemic wave, in order to reduce the endemic burden and exterminate the disease eventually. In Indian perspective, one can use the factor of migrant laborers. One may develop the model with the use of stochastic, fuzzy and intuitionistic fuzzy uncertainties.

Acknowledgements

The first author would like to acknowledge the financial support by DST-INSPIRE, Government of India, Ministry of Science & Technology, New Delhi, India (DST/INSPIRE-Fellowship/2017/IF170211).

References

- [1] Anderson R M, May R M (1986): The invasion, persistence and spread of infectious diseases within animal and plant communities. Philosophical transaction of the Royal Society of London. Series B, Biological sciences, 314: 533–570, 1986.
- [2] Carcione J M, Santos J E, Bagaini C, Ba J (2020): A Simulation of a COVID-19 Epidemic Based on a Deterministic SEIR Model. Front. Public Health. <https://doi.org/10.3389/fpubh.2020.0230>.
- [3] Ding Y, Gao L (2020): An evaluation of COVID-19 in Italy: A data-driven modeling analysis. Infectious Disease modelling. <https://doi.org/10.1016/j.idm.2020.06.007>.

- [4] Birkhoff G, Rota, G C, Ordinary Differential Equation (Ginn, Boston, 1982).
- [5] Cai Y, Kang Y, Wang W. A stochastic SIRS epidemic model with nonlinear incidence rate. *Appl Math Comput Elsevier Inc.*; 2017; 305: 221–40. Available from: <http://dx.doi.org/10.1016/j.amc.2017.02.003>.
- [6] Chavez C C, Feng Z, Mathematical models for the disease dynamics of tuberculosis. BU-1321M, 1996.
- [7] Chang Z, Meng X, Lu X. Analysis of a novel stochastic SIRS epidemic model with two different saturated incidence rates. *Phys A Stat Mech its Appl Elsevier B.V.*; 2017; 472: 103–16. Available from: <http://dx.doi.org/10.1016/j.physa.2017.01.015>.
- [8] Chen S H, Hsieh CH. Graded mean integration representation of generalized fuzzy number. 1999 Diekmann O, Hstereebek JAP, Roberts M G, The construction of next-generation matrices for compartmental epidemic models, *J. R. Soc. Interface*, (doi:10.1098/rsif.2009.0386), 2009.
- [9] Dobson A, Foufopoulos J. Emerging infectious pathogens of wildlife. *Philosophical transaction of the Royal Society of London. Series B, Biological sciences*, 365: 1001–1012, 2001.
- [10] Efimov D, Ushirobira R, Efimov D, Ushirobira R. On an interval prediction of COVID-19 development based on a SEIR epidemic model To cite this version: HAL Id: hal-02517866 On an interval prediction of COVID-19 development based on a SEIR epidemic model. 2020.
- [11] Giordano G, Blanchini F, Bruno R, Colaneri P, Fillippo AD, Matteo AD, Colaneri M, Modelling the COVID-19 epidemic and implementation of population-wide interventions in Italy. <https://doi.org/10.1038/s41591-020-0883-7>, 2020.
- [12] Grenfell B T, Dobson A P. *Ecology of Infectious Disease in Natural Populations*. Cambridge University Press, Cambridge, 1995.
- [13] Hethcote HW. *SIAM Rev* 2000; 42: 599.
- [14] Hudson P J, Rizzoli A, Grenfell B T, Heesterbeek H, Dobson AP. *Ordinary Differential Equation. The Ecology of Wildlife Diseases*. Oxford University Press, Oxford, 2001.
- [15] Musa S S, Qureshi S, Zhao S, Yusuf A, Mustapha UT, He D (2021): Mathematical modelling of COVID-19 epidemic with effect of awareness programs. *Infect Dis Model*. doi: 10.1016/j.idm.2021.01.012.
- [16] Liu Z, Magal P, Seydi O, Webb G (2020): A COVID-19 epidemic model with latency period. *Infectious Disease Modelling*. <https://doi.org/10.1016/j.idm.2020.03.003> <https://www.who.int/emergencies/diseases/novel-coronavirus-2019>
- [17] Imai N, Cori A, Dorigatti I, Baguelin M, Donnelly C A, Riley S, Ferguson NM, Report 3: transmissibility of 2019-ncov. Reference Source, 2020.
- [18] John Hopkins Hospital (JHH), Coronavirus COVID-19 Global Cases by the Center for Systems Science and Engineering (CSSE) at Johns Hopkins. Accessed by March 14, 2020 on: <https://www.arcgis.com/apps/opsdashboard/index.html/bda7594740fd40299423467b48e9ecf6>.
- [19] Khajanchi S, Sarkar K (2020): Forecasting the daily and cumulative number of cases for the COVID-19 pandemic in India. *Chaos* 30, 071101; <https://doi.org/10.1063/5.0016240>, 2020.
- [20] Khan A M, Gomez-Aguilar J F. Tuberculosis model with relapse via fractional conformable derivative with power law. *Math Methods Appl Sci* 2019; 42(18). <https://doi.org/10.1002/mma.5816>.
- [21] Khan M A, Ullah S, Farhan M. The dynamics of Zika virus with Caputo fractional derivative. *AIMS Math* 2019; 4(1): 134–46. <https://doi.org/10.3934/Math.2019.1.134>.
- [22] Khan A, Gomez-Aguilar J F, Khan T S, Khan H. Stability analysis and numerical solution of fractional order HIV/AIDS model. *Chaos, Solitons Fractals* 2019; 122. <https://doi.org/10.1016/j.chaos.2019.03.022>.
- [23] Kermack W O, McKendrick A G, A Contribution to the Mathematical Theory of Epidemics. *Proceedings of the Royal Society*. 115(772): 700–722, 1927.
- [24] Kamrujjaman M, Mahmud M S, Islam M S, Coronavirus Outbreak and the Mathematical Growth Map of COVID-19. *Annual Research & Review in Biology*. 35(1): 72–78, 2020.
- [25] Krebs C J. Two paradigms of population regulation. *European Journal of Wildlife Research*, 22: 1–10, 1995.
- [26] Lahrouz A, Omari L, Kiouach D. Global analysis of a deterministic and stochastic nonlinear SIRS epidemic model. *Nonlinear Anal Model Control* 2011; 16: 59–76.
- [27] Lega J, Brown H E. Data-driven outbreak forecasting with a simple nonlinear growth model. *Epidemics* 2016; 17: 19e26.
- [28] Lipsitch M, Ted C, Ben C, et al. Transmission dynamics and control of severe acute respiratory syndrome. *Science* 2003; 300: 1966–70.
- [29] Mahata A, Mondal S P, Ahmadian A, Ismail F, Alam S, Salahshour S. Different Solution Strategies for Solving Epidemic Model in Imprecise Environment. *Complexity* 2018; 2018.
- [30] May R M. Conservation and disease. *Conservation Biology*, 2: 28–30, 1988.
- [31] Murray J D. *Mathematical Biology*. Berlin: Springer; 1993.

- [32] Ming W K, Huang J, Zhang C J, Breaking down of Healthcare System: Mathematical Modeling for Controlling the Novel Coronavirus (2019-nCoV) Outbreak in Wuhan, China. *bioRxiv*, 2020.
- [33] Nandi S K, Jana S, Manadal M, Kar T K. Analysis of a fuzzy epidemic model with saturated treatment and disease transmission. *Int J Biomath* 2018; 11.
- [34] Nesteruk I, Statistics Based Predictions of Coronavirus 2019-nCoV Spreading in Mainland China. *MedRxiv*, 2020.
- [35] Nishiura H, Endo A, Saitoh M, et al. Identifying determinants of heterogeneous transmission dynamics of the Middle East respiratory syndrome (MERS) outbreak in the Republic of Korea, 2015: a retrospective epidemiological analysis. *BMJ Open* 2016; 6(2): 1012–33.
- [36] Njankou, S. D. D., Nyabadza, F.: An optimal control model for Ebola virus disease. *J. Biol. Syst.* 24, 1–21 (2016).
- [37] Oduwole H K, Kimbir A R, “Modelling vertical transmission and the effect of Antiretroviral Therapy (ART) on the dynamics of HIV/AIDS in an age-structured population in Nigeria. *Journal of Natural and Applied Science-Nasara Scientifique*, Vol. 7 No. 1 pp. 51–78, 2018.
- [38] Mahato P, Das S, Mahato S K An epidemic model through information induced vaccination and treatment under fuzzy impreciseness. *Modeling Earth Systems and Environment* (2021) <https://doi.org/10.1007/s40808-021-01257-7>.
- [39] Pal D, Ghosh D, Santra P K, Mahapatra G S, Mathematical Analysis of a COVID-19 Epidemic Model by using Data Driven Epidemiological Parameters of Diseases Spread in India, 2020.
- [40] Pell B, Kuang Y, Viboud C, Chowell G. Using phenomenological models for forecasting the 2015 Ebola challenge. *Epidemics* 2018; 22: 62e70.
- [41] Riley S, Christophe F, Donnelly C, et al. Transmission dynamics of the etiologic agent of SARS in Hong Kong: impact of public health interventions. *Science* 2003; 300: 1961–6.
- [42] Santillana M, Tuite A, Nasserie T, Fine P, Champredon D, Chindelevitch L, et al. Relatedness of the incidence decay with exponential adjustment (IDEA) model, “Farr’s law” and SIR compartmental difference equation models. *Infectious Disease Modelling* 2018; 3: 1e12.
- [43] Suttle C, Chan A, Cottrell M. (1990): Infection of phytoplankton by viruses and reduction of primary productivity. *Nature*, 347: 467–469, <https://doi.org/10.1101/2020.04.25.20079111>.
- [44] Tang B, Wang X, Li Q, Bragazzi N L, Tang S, Xiao Y, Wu J (2020): Estimation of the transmission risk of the 2019-nCoV and its implication for public health interventions. *Journal of Clinical Medicine*, 9(2): 462, 2020.
- [45] Van den Driessche P, Watmough J, Reproduction numbers and sub-threshold endemic equilibria for compartmental models of disease transmission. *Math. Biosci.* 180, 29–48, doi: 10.1016/S0025-5564(02)00108-6, 2002.
- [46] Victor A O, Oduwole H K, Evaluating the Deterministic SEIRUS Model for Disease Control in an Age-Structured Population. *Global Scientific Journal*. Preprint, 2020.
- [47] World Health Organization. The world health report 2004: changing history. World Health Organization, 2004.
- [48] Wu J T, Leung K, Leung G M Nowcasting and Forecasting the Potential Domestic and International Spread of the 2019-nCoV Outbreak Originating in Wuhan, China: a Modeling Study. *The Lancet*, 395(10225): 689–697, 2020.
- [49] Zadeh. L A. Fuzzy sets. *Inf. Control.* 8, 338–353, 1965.
- [50] Purkayastha S, Bhattacharyya R, Bhaduri R (2021): A comparison of five epidemiological models for transmission of SARS-CoV-2 in India. *BMC Infect Dis* 21, 533. <https://doi.org/10.1186/s12879-021-06077-9>.
- [51] Saikia D, Bora K, Bora M P (2021): COVID-19 outbreak in India: an SEIR model-based analysis. *Nonlinear Dyn.* Doi: 10.1007/s11071-021-06536-7
- [52] Pontryagin L S, Boltyanskii V G, Gamkrelidze R V, Mishchenko E F (1962): *The Mathematical Theory of Optimal Processes* (Wiley, New York, 1962).
- [53] Das S, Mahato P, Mahato S K (2020): A Prey Predator in Case of Disease Transmission via Pest in Uncertain Environment, *Differ Equ Dyn Syst*, 1–27. <https://doi.org/10.1007/s12591-020-00551-7>.
- [54] Das S, Mahato P, Mahato S K Disease control prey-predator model incorporating prey refuge under fuzzy uncertainty. *Model. Earth. Syst. Environ.* 7(4), 2149–2166 (2021). <https://doi.org/10.1007/s40808-020-00892-w>.
- [55] Das S, Mahato P, Mahato S K, Pal D (2021): A Mathematical Study of Pandemic COVID-19 Virus with Special Emphasis on Uncertain Environment. *Journal of Applied Nonlinear Dynamics* 11(2) (2022) 427–457. DOI: 10.5890/JAND.2022.06.012
- [56] Das S, Mahato P, Mahato S K (2021): Biological control of infection pervasive via pest : a study of prey-predator model incorporating prey refuge under fuzzy impreciseness, *Int J Model Simul* (2021). <https://doi.org/10.1080/02286203.2021.1964060>.